JOURNAL OF VIROLOGY, Dec. 2004, p. 12951–12963 Vol. 78, No. 23
0022-538X/04/$08.00+0 DOI: 10.1128/JVI.78.23.12951–12963.2004

Two Modes of Pseudorabies Virus Neuroinvasion and Lethality in Mice

Elizabeth E. Brittle, Ashley E. Reynolds, and L. W. Enquist*

Department of Molecular Biology, Princeton University, Princeton, New Jersey

Received 17 June 2004/Accepted 6 August 2004

We describe two distinct modes of neuroinvasion and lethality after murine flank inoculation with virulent and attenuated strains of pseudorabies virus (PRV). Mice infected with virulent (e.g., PRV-Becker, PRV-Kaplan, or PRV-NIA3) strains self-mutilate their flank skin in response to virally induced pruritus, die rapidly with no identifiable symptoms of central nervous system (CNS) infection such as behavioral abnormalities, and have little infectious virus or viral antigen in the brain. In distinct contrast, animals infected with an attenuated PRV vaccine strain (PRV-Bartha) survive approximately three times longer than wild-type PRV-infected animals, exhibit severe CNS abnormalities, and have an abundance of infectious virus in the brain at the time of death. Interestingly, these animals have no skin lesions and do not appear pruritic at any time during infection. The severe pruritus and relatively earlier time until death induced by wild-type PRV infection may reflect the peripheral nervous system (PNS) and immune responses to infection rather than a fatal, virally induced CNS pathology. Based on previously characterized afferent (sensory) and efferent (motor) neuronal pathways that innervate the skin, we deduced that wild-type virulent strains transit through the PNS via both afferent and efferent routes, whereas PRV-Bartha travels by only efferent routes in the PNS en route to the brain.

Pseudorabies virus (PRV), a swine alphaherpesvirus, is a member of the alphaherpesvirus subfamily, including human and animal pathogens such as varicella-zoster virus, herpes simplex virus type 1 (HSV-1) and HSV-2, bovine herpesvirus types 1 and 5, and equine herpesviruses types 1 and 4 (23). Although the natural hosts of PRV are adult swine, PRV is pantropic, infecting avian embryos and a wide range of mammalian species, with the notable exceptions of humans and other higher-order species of nonhuman primates.

PRV routinely establishes a latent infection in PNS ganglia of adult swine and yet rarely invades the central nervous systems (CNS) of these animals (8). Viral spread between adult swine occurs primarily via direct mucosal contact. Common sequelae of wild-type PRV infection include respiratory disease, weight loss, and infertility in pregnant gilts and sows (31). In contrast, PRV infection is lethal in neonatal piglets and in nonnative hosts such as cows, dogs, rodents, and other susceptible animals. In these animals, infection induces severe, uncontrollable pruritus (itchiness), culminating in frantic self-mutilating behavior historically described as "mad itch." Death ensues within days of infection with virulent strains of PRV. The cause of death of these animals has traditionally been ascribed to fatal encephalitis.

Adult swine infected with live, attenuated vaccine strains such as PRV-Bartha typically exhibit few, if any, symptoms of infection. In addition, most attenuated PRV strains are significantly less virulent in nonnative hosts such as rodents (8). Despite the attenuated phenotype, PRV-Bartha remains neuroinvasive in nonnative hosts and can cause massive brain infections. The combined properties of neuroinvasiveness and reduced virulence enable neuroanatomists to utilize PRV-Bartha and recombinant Bartha strains as tracers of neuronal connections in many laboratory animals (10).

Several lines of evidence indicate that PRV-Bartha is neuroinvasive but can spread only in the retrograde direction in a neuronal circuit (from postsynaptic to presynaptic neurons) (8, 20). Spread of infection of wild-type virus in the anterograde direction (from presynaptic to postsynaptic neurons) requires the PRV U_S9, gE, and gI proteins (4, 12). These genes are deleted in the PRV-Bartha strain (3, 14, 16, 18, 19, 22). The U_S9, gE, and gI gene products are not required for spread in the retrograde direction. In addition, in virulent PRV strains, the gE and gI proteins play significant roles in promoting the characteristic symptoms of PRV infection and rapid death (32).

We used a flank scarification method of PRV inoculation previously described for other alphaherpesviruses (24, 25). The mouse flank infection model emulates a naturally occurring alphaherpesvirus infection in that infection is initiated in epithelial tissue, followed by spread of virus to the PNS, with the potential for further progression into structures of the CNS. The neuronal pathways innervating the skin are well characterized in the mouse. In addition, the intrinsic cellular defense mechanisms and innate immune responses are robust in the skin. These features enable relatively facile assessment of the roles of viral gene products in virulence. Moreover, unlike infection models involving tissues of the head and neck, no cranial nerves can be directly infected from flank skin, a property that enables better assessment of neuroinvasiveness.

We report that infection with virulent PRV infection of a single site on the mouse right flank results in frantic scratching and biting of the skin at the inoculation site, as well as the corresponding dermatome. Self-induced trauma to the skin

* Corresponding author. Mailing address: 314 Schultz Laboratory, Department of Molecular Biology, Princeton University, Princeton, NJ 08544. Phone: (609) 258-2415. Fax: (609) 258-1035. E-mail: lenquist@molbio.princeton.edu.

TABLE 1. Genotypes of PRV strains

Strain	Genotype	Reference(s)
PRV-Becker	PRV wild type	13
PRV-Kaplan	PRV wild type	13
NIA3	PRV wild type	13
PRV-160	Us9 null	4
PRV-91	gE null	7
PRV-98	gI null	30
PRV-Bartha	Δ(gI-gE-Us9, Us2), point mutations in gC, U_L21, gM	3, 14, 16, 18, 19, 22
PRV-158	PRV-Bartha with Us9, gE, and gI restored	17
PRV-BaBe	Δ(gI-gE-Us9, Us2) isogenic with PRV-Becker	7

culminates in the development of a dramatic, but extremely precise, dermatome lesion at the infection site. Mice infected with wild-type PRV become progressively weaker and die at approximately 75 h postinfection with no detectable behavioral abnormalities indicative of CNS pathology and virtually undetectable amounts of virus in the brain. In contrast, mice inoculated on the flank with the attenuated strain PRV-Bartha exhibit dramatically different features. Although these animals ultimately die, they survive nearly three times longer than those infected with wild-type PRV. They do not become pruritic and do not develop skin lesions of any kind during the course of infection, despite viral replication in the skin and corresponding ganglia. PRV-Bartha-infected mice remain asymptomatic until ~140 h, at which time they develop frank neurological abnormalities such as ataxia. The animals die approximately at 220 h with an abundance of virus in brain tissue. This model delineates two distinct modes of lethality depending on the virulence of the infecting strain. Importantly, dramatic differences between PRV-Becker and PRV-Bartha enable careful dissection of the functions of specific PRV-encoded genes essential for pathogenesis.

MATERIALS AND METHODS

Reagents. All chemicals were purchased from Sigma unless noted otherwise.

Virus strains. PRV-Becker is a virulent laboratory strain. The isogenic strains PRV-91 (gE-null), PRV-98 (gI-null), and PRV-160 (U_S9-null) (deletions of the gE, gI, and U_S9 genes, respectively) were previously described (4, 7, 30) (referenced in Table 1). The genome of the attenuated vaccine strain PRV-Bartha encodes a number of mutations, including deletion of a region of the unique short (U_S) region of the PRV genome, including the genes encoding U_S9, gE, gI, and U_S2 (described in detail elsewhere [3, 14, 16, 18, 19, 22]). Two additional virulent strains, PRV-Kaplan and PRV-NIA3, used for these studies have been described elsewhere (13). Propagation and plaque assay of all PRV strains were performed utilizing PK15 (pig kidney) cells.

Antisera. The PRV-specific rabbit antiserum RB133 (diluted 1:7,000) utilized for immunohistochemical analysis was described previously (7).

Mouse flank infection protocol. Experimental protocols for these studies were approved by the Princeton University Animal Welfare Committee and Office of Research and Project Administration. Animal use protocols were fully compliant with the regulations established by the American Association for Accreditation of Laboratory Animal Care and the stipulations of the Animal Welfare Act (Public Law 99-198). The mouse flank infection experiments were performed with 6- to 7-week-old female C57BL/6/J mice (Jackson Laboratories). Upon arrival at Princeton University, the 5- to 6-week-old mice were allowed to acclimate in the Princeton University Biosafety Level Two Animal Housing Facility for 1 week before the experiments began. During the acclimation period and throughout the course of the experiment, the mice were maintained under constant ambient temperature and photoperiod conditions (12 h of light, 12 h of darkness). The protocol used for the mouse flank inoculation was adapted from the protocol described by Simmons and Nash (25) and Friedman and coworkers (24, 29). The mice each weighed ~17 g and were anesthetized with an intraperitoneal (i.p.) injection of a 100-μl total volume of filter-sterilized 14.3-mg/ml

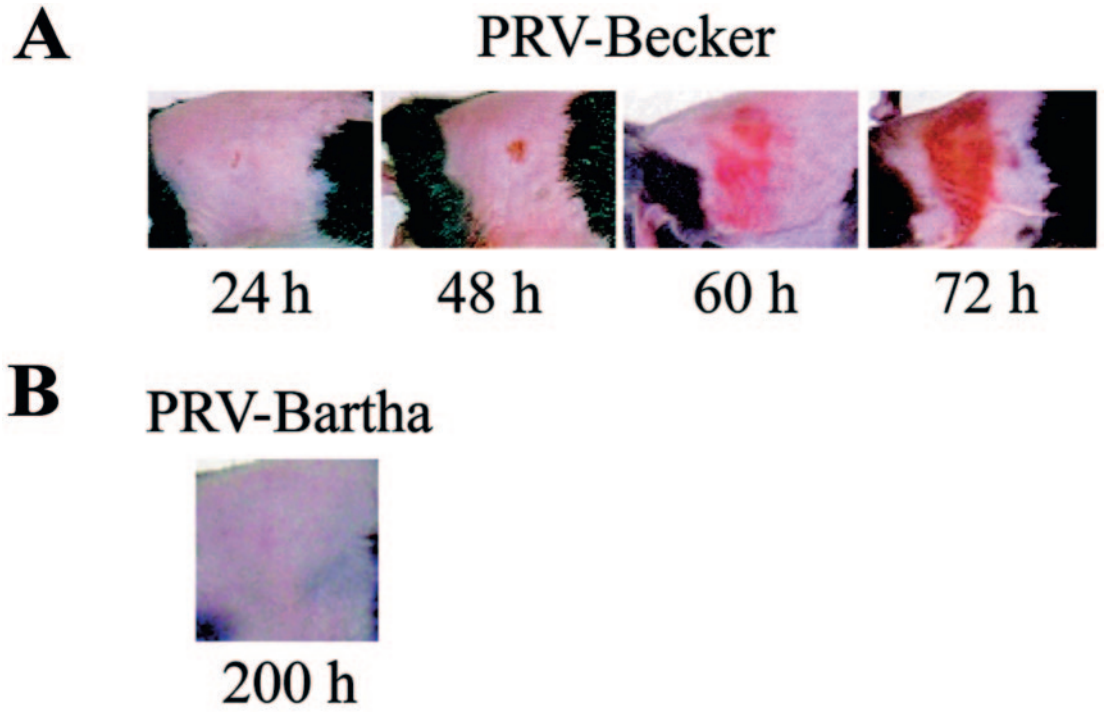

FIG. 1. (A) Development and progression of the erythematous dermatome lesions observed in virulent PRV mouse flank infections. Mice were infected as described in Materials and Methods with PRV-Becker. Representative images of mice at 24, 48, 60, and 72 h are depicted. (B) Representative image of a PRV-Bartha-infected mouse at 200 h.

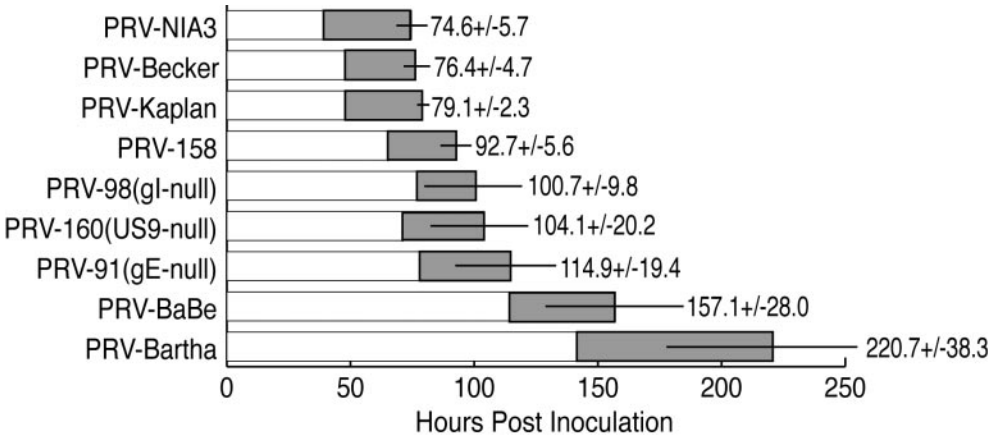

FIG. 2. Time until death postinfection of mice infected with strains of PRV. Mice were infected via flank scarification and then observed as described in Materials and Methods. A sample set of seven mice was inoculated with each strain. The shaded area of each bar indicates the period of time in which symptoms were apparent. The horizontal line indicates the standard deviation.

ketamine and 1.8-mg/ml xylazine diluted into phosphate-buffered saline (PBS; Gibco). Once anesthetized, the animals were placed in left lateral recumbency; hair was removed from the paravertebral fossa region, the depressed region of the flank cranial to the hip. After clipping, depilatory cream (Nair) was applied for 2 min to the right flank region. The cream was then removed with soft, clean gauze and copious volumes of water. Approximately 48 h later, the mice were reanesthetized by i.p. injection of the ketamine and xylazine prepared as described above.

Once anesthetized, a 10-μl droplet of inoculum containing 10^6 PFU of PRV suspended in viral medium (Dulbecco modified Eagle medium plus 2% fetal bovine serum [Gibco]) was applied to the hairless, right paravertebral fossa region. To facilitate adsorption of virus, the stratum corneum underlying the droplet was disrupted by lightly scratching the skin 40 times in four different directions (10 times in the horizontal direction, 10 times in the vertical direction, 10 times along the right diagonal, and 10 times along on the left diagonal) with a sterile 25-gauge needle.

The mice were carefully observed every 6 to 8 h throughout the course of the experiments. A standardized checklist enabled accurate documentation of key experimental parameters, including the overall demeanor of the animals, skin appearance at the site of inoculation and corresponding dermatome, appetite, pruritus, gait disturbances, and the time of death postinfection.

Anesthesia studies. Beginning at 40 h after infection and extending until 60 h, PRV-Becker infected mice were anesthetized with a ketamine-xylazine cocktail at the dosages described above every 2 to 4 h. This treatment effectively rendered the animals unconscious or significantly sedated for periods of 1 to 2 h during the course of infection at time points when the untreated animals were scratching frantically.

Recovery of infectious virus from tissues. For plaque-forming assays, tissues were harvested from mice immediately after the animals were euthanized in a carbon dioxide chamber at 36, 72, 96, 168, and 236 h after inoculation. Tissues dissected from the mice included: two 8-mm circular skin punches from both the site of inoculation and a ventral, secondary site within the same dermatome region, ipsilateral dorsal root ganglia (DRG), spinal cord, hindbrain, and the left and right cerebral hemispheres. Three mice were infected for each data point, and similar tissues were pooled in preweighed sterile Eppendorf tubes. Tissue samples were weighed, 500 μl of Dulbecco modified Eagle medium–2% fetal bovine serum was added, and the tissues were flash frozen by immersion of the Eppendorf tube in liquid nitrogen and then stored at −80°C until titers were determined. To enumerate the number of viral PFU per gram of tissue, samples were warmed to 37°C and homogenized by using a sterile disposable pestle (Kontes). The tissue homogenates were treated with two additional cycles of flash freezing by immersion of tubes in liquid nitrogen and rapid thawing to 37°C. The homogenates were centrifuged at 3,000 × *g* in a microfuge for 5 min. The clarified supernatant was transferred to a fresh Eppendorf tube, and the relative PFU titers in the respective tissues were determined on monolayers of PK15 cells.

In a separate experiment, the following organs were removed: lungs, heart, liver, spleen, pancreas, kidneys, adrenal glands, stomach (emptied of contents), ovaries, uterus, and urinary bladder. The same organs from sets of three mice were pooled and prepared as described above with the additional step of pulverizing tissues with a motorized tissue grinder (sterilized with 100% ethanol and rinsed between each sample).

Tissue perfusion, sectioning, and immunohistochemistry. At various times postinfection, mice were sacrificed and exsanguinated by transcardiac perfusion of a 15-ml bolus of ice-cold 4% (wt/vol) paraformaldehyde-PBS. After 5 min, animals were perfused with an additional 15 ml of the cold paraformaldehyde-PBS solution as described above. The brains were carefully dissected and placed in 4% paraformaldehyde-PBS at 4°C for 24 h. Subsequently, brains were cryoprotected via sequential immersion for 24-h time periods in sterile-filtered 10, 20,

TABLE 2. LD_{50} values for PRV-Becker and PRV-Bartha in the flank model

Strain	LD_{50} (PFU)	Avg survival time (h)[a] (*n*)
PRV-Becker	1.47×10^4	86.6 (14)
PRV-Bartha	7.4×10^5	221.2 (12)

[a] *n,* Number of mice.

TABLE 3. Lesion severity at death induced by PRV strains

Strain	*n*[a]	Lesion severity (%)[b]			
		Severe	Moderate	Mild	No lesion
PRV-Becker	25	100	0	0	0
Kaplan	7	100	0	0	0
NIA3	7	100	0	0	0
PRV-158	7	100	0	0	0
PRV-98 (gI null)	7	42.9	14.3	28.6	14.3
PRV-160 (Us9 null)	21	14.3	42.9	42.9	0
PRV-91 (gE null)	25	8.0	28.0	56.0	8.0
PRV-BaBe	7	14.3	28.6	28.6	28.6
PRV-Bartha	25	0	0	0	100

[a] That is, the total number of mice (*n*) used in these calculations.

[b] The percentage values were calculated by dividing the number of animals falling into a particular category by the total number of animals observed and then multiplying that value by 100. The lesion severity was classified as follows: severe = red, fully crusted dermatome lesion with stiff, rough texture; moderate = dermatome lesion with combination of smooth redness and rough texture; mild = redness along dermatome (or at primary site of inoculation only) with little change in skin texture; and no lesion = no change from normal skin color or texture.

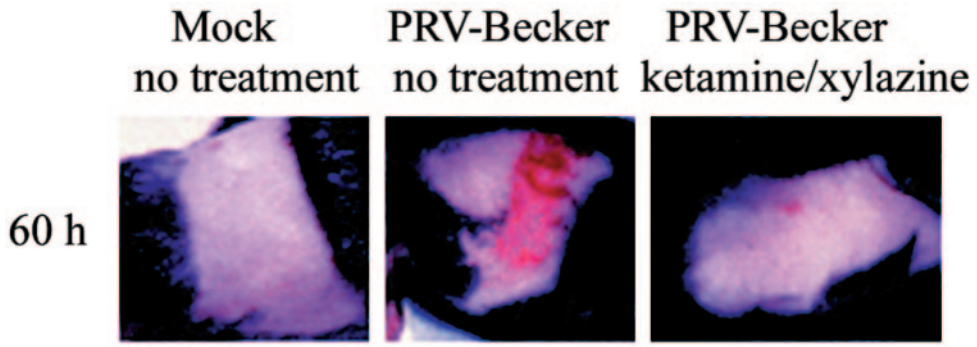

FIG. 3. Images of mouse flanks mock infected or infected with PRV-Becker at 60 h. Mock-infected mice received no anesthesia (no treatment). PRV-Becker-infected mice were either not anesthetized (no treatment) or were anesthetized by i.p. injection at regular intervals from 40 to 60 h with ketamine and xylazine (ketamine/xylazine).

and 30% (wt/vol) sucrose (Roche) diluted in 4°C PBS. Coronal sections (~40 μm thick) of the perfused tissue were generated by using a freezing microtome. Sections were processed and stained as described by Card and Enquist (5).

RESULTS

Distinctive symptoms of virulent PRV flank infection. In contrast to the HSV skin lesions described by Simmons and Nash (25) as mild, with the appearance of zosteriform vesicular lesions, PRV-induced skin lesions are not vesicular but instead are florid with evidence of overt tissue damage. Symptoms became apparent about 40 h after infection with the virulent PRV-Becker strain. The predominant features were severe pruritus, inducing the animals to frantically claw and bite the right flank region, rolling, and unwillingness to bear weight on the right hind limb. The pruritus escalated in severity until the animals directed the entirety of their energy to scratching and biting the site of viral inoculation and a precise, belt-like region encompassing the site of infection, strictly on the right (ipsilateral) side. Soon after development of pruritus, the skin appeared pink and shiny. This appearance gradually progressed to a severe, erythematous, crusted dermatome lesion as seen in Fig. 1A. The lesions were confined to one or more overlapping dermatomes predicted to encompass the fields of sensory neurons that innervate the site of primary infection. Animals infected with PRV-Becker died, on average, at 76.4 h with a standard deviation of <5 h (Fig. 2). Approaching the time of death, the animals no longer displayed signs of pruritus, were unresponsive to external stimuli, sat with hunched body posture, had dull, sunken eyes, and a piloerected, rough fur coat. Before death, the mice were moribund and exhibited agonal breathing.

PRV-Bartha is markedly attenuated compared to virulent PRV strains. (i) Mean survival time. The survival times of three different wild-type virulent PRV strains were compared directly to that of the attenuated vaccine strain, PRV-Bartha. Mice infected with three virulent strains utilized in these studies, Becker, Kaplan, and NIA3, had mean survival times of 76.4, 79.1, and 74.6 h, respectively (Fig. 2). The standard deviation was <6 h for these strains. In contrast, mice infected with PRV-Bartha survived an average of 220.7 h, nearly three times the survival time of animals infected with virulent strains. As survival time increased, the range between the first death and the last death for a group infected with a particular strain generally increased. At the two extremes were infections with PRV-Kaplan, which had a standard deviation of time until death of 2.3 h and PRV-Bartha, which had a standard deviation of 38.3 h.

(ii) LD_{50}. The 50% lethal dose (LD_{50}) calculations were based on the equation of Reed and Muench (21). The LD_{50} for PRV-Bartha was 7.4×10^5 PFU, and the LD_{50} for PRV-Becker was 1.47×10^4 PFU (Table 2). The average survival time for PRV-Becker infected mice increased from 82.0 h, with an inoculating dose of 10^6 PFU, to 90.4 h when 10^5 PFU were used for inoculation. The average survival time for PRV-Bartha-infected animals did not vary significantly, with an inoculating dose of 10^7 PFU resulting in an average survival time of 217.6 h and a dosage of 10^6 PFU resulting in an average survival time of 215.8 h.

PRV-Bartha does not cause pruritus. The characteristic lesions and pruritus exhibited by mice infected with the virulent PRV strains, NIA3 and Kaplan, were as severe as those observed for PRV-Becker (Table 3). In marked contrast, PRV-Bartha-infected animals displayed absolutely no pruritus at any time during infection and exhibited no skin lesions (Fig. 1B). Beginning at ca. 140 h, PRV-Bartha-infected animals did, however, display behavioral abnormalities such as ataxia, gait disturbances, and tremors.

Analysis of selected PRV-Becker mutants enabled an assignment of PRV genes responsible for PRV virulence. The genome of PRV-Bartha contains point mutations in the genes encoding gC, U_L21 and gM, as well as a deletion of several kilobase pairs in the U_S region. The deletion in the U_S region of the Bartha genome removes the coding sequences for U_S9 protein, as well as gE, gI, and U_S2 proteins (3, 14, 16, 18, 19, 22). To determine the relative contributions of these genes to virulence in our studies, we infected mice with Becker isogenic strains, PRV-160 (U_S9-null), PRV-91 (gE-null), and PRV-98 (gI-null), which carry deletions in the genes encoding U_S9, gE, and gI, respectively. These three viral proteins, U_S9, gI, and gE, significantly impact the pathogenesis of PRV when studied in other animal model systems such as the rodent eye model (reviewed in reference 9). Flank infections with PRV-98 (gI-null), PRV-160 (U_S9-null), and PRV-91 (gE-null) resulted in mild to moderate lesions (Table 3) and mean survival times of 100.7, 104.1, and 114.9 h, respectively (Fig. 2). Infection by mutants lacking any one of these three genes had modest effects on symptoms. The trend of the results suggests that

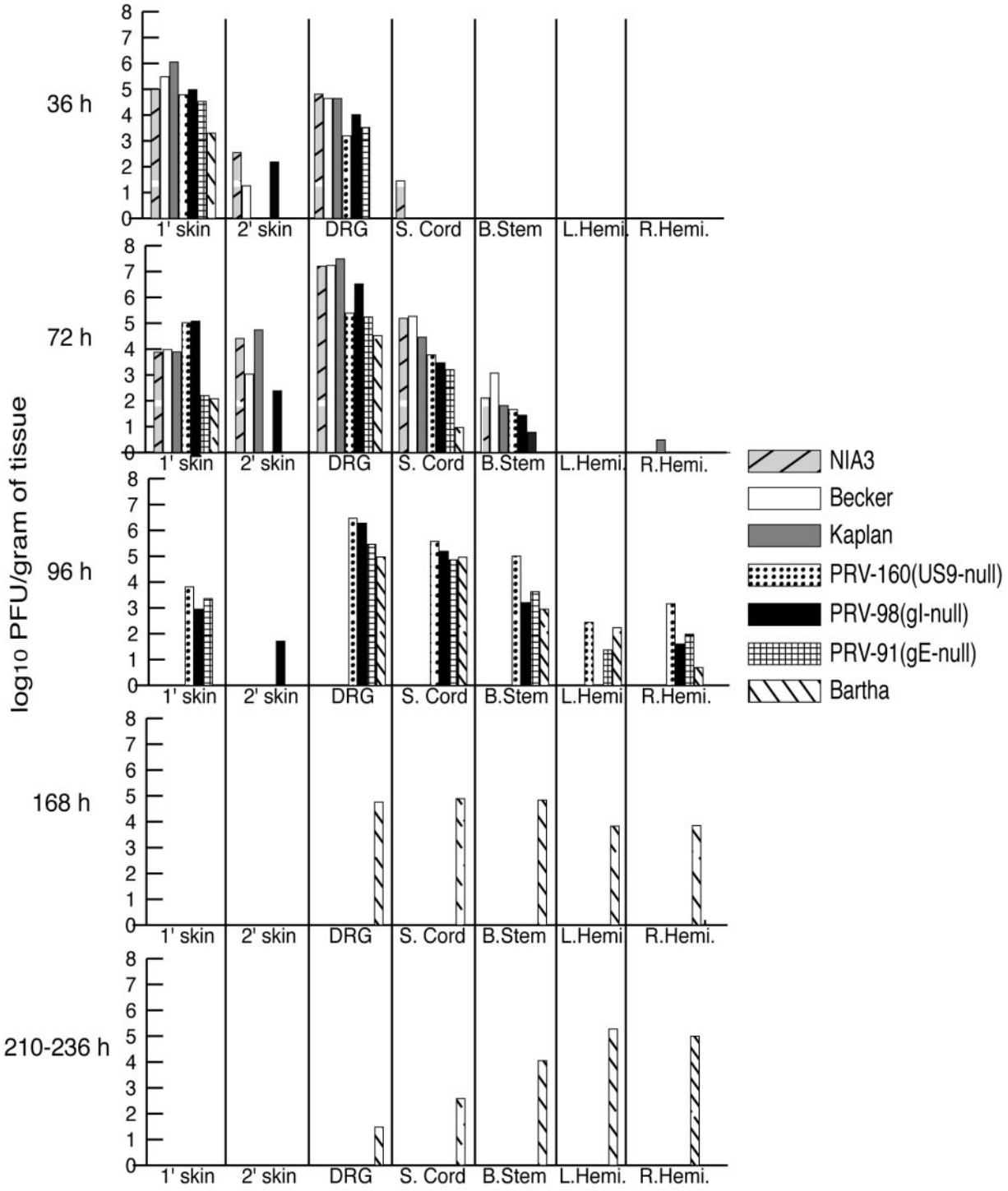

FIG. 4. Titration of infectious virus from infected tissues over time. Mice were infected with each PRV strain, and tissues were processed as described in Materials and Methods. Three mice per strain per time point were inoculated. Mice were sacrificed, and tissues were collected from mice inoculated with each virus at 36 and 72 h. At 96 h, mice inoculated with PRV-160 (U_S9 null), PRV-98 (gI null), PRV-91 (gE null), and PRV-Bartha were sacrificed, and tissues were harvested for virus isolation. Tissues from four mice in two separate experiments were collected from PRV-Bartha-infected mice at 168 h and 210 to 236 h, respectively. Strains at time points exceeding the time until death postinoculation were necessarily omitted.

deletion of gE results in the longest survival time of the animals and the greatest attenuation of symptoms.

In order to understand the combined effect of gE, gI, and U_S9 on PRV virulence, groups of mice were infected with either PRV-158 (PRV-Bartha with the U_S region restored) or PRV-BaBe (a strain isogenic with PRV-Becker with the U_S deletion of PRV-Bartha) (Table 1). Inoculation of PRV-158 yielded an average time to death of 92.7 h, with all mice

TABLE 4. Recovery of infectious virus from various organs

Organ	Recovery (log_{10}[PFU/g]) of:	
	PRV-Becker at 70 h	PRV-Bartha at 192 h
Heart	0.8	2.0
Lungs	0.2	<0.4
Kidneys	4.9	0.2
Liver	<−0.5	<−0.4
Adrenal glands (both)	7.6	3.5
Ovaries	7.0	<2.0
Spleen	<0.7	<0.7
Pancreas	3.0	<0.5
Stomach	<0.5	<0.5
Urinary bladder and uterus	5.3	1.4

developing severe dermatome crusts and symptoms identical to those associated with PRV-Becker infection. The time of onset of symptoms of PRV-158-infected mice was delayed by ~24 h relative to PRV-Becker. PRV-BaBe-infected mice died at an average time of 157 h, with approximately two-thirds of the mice developing pruritus and mild to moderate dermatome lesions (Table 3). The remaining third of the population of PRV-BaBe-infected mice developed a phenotype comparable to PRV-Bartha-infected mice in that they showed CNS abnormalities prior to death and showed no skin lesions or pruritus. These results indicated that the absence of the genes encoding U_S9, gE, and gI in PRV-Bartha accounts for much, but not all, of its attenuation.

Erythematous dermatome lesions on the flanks of PRV-infected mice result from self-mutilation. The unilateral lesions on the flanks of PRV-Becker-infected mice were in a precise dermatome pattern (Fig. 1). We postulated that the lesions could be attributed to two possible causes: (i) viral replication in the skin resulting in necrosis or (ii) self-mutilating behavior such as biting and scratching the skin flank stimulated by viral infection. To distinguish between these possibilities, mice were infected with PRV-Becker and a subset were put under general anesthesia at regular intervals. Anesthetized animals could not traumatize the flank region during the anesthesia period. If the lesions were due to viral replication in the skin, the lesions in the untreated mice should be identical to those in the anesthetized mice. However, if the lesions were due to self-mutilation, the lesions would be significantly diminished in the anesthetized animals compared to the conscious infected animals.

The results were unequivocal. At late time points postinfection such as 60 h, the anesthetized mice exhibited significantly milder flank lesions than the nonanesthetized mice (Fig. 3). Interestingly, although the animals appeared sedated and lethargic upon recovery from anesthesia, they inevitably immediately began scratching and biting their skin. This accounts for the mild lesions shown in Fig. 3, right panel. This behavior underscores the intensity of the internal stimulus driving the animals to excoriate the flank skin. We conclude that the florid lesions reflect self-mutilation and do not represent the effects of virus replication in the skin. Importantly, regardless of whether the animals were anesthetized, the average time until death in the PRV-Becker-infected animals was approximately 76 h. It is clear that the self-mutilation and severe lesions had little to no influence on time to death. The observation that lesions were markedly less severe in PRV-98 (gI-null)-, PRV-160 (U_S9-null)-, and PRV-91 (gE-null)-infected animals indicates that the gI, U_S9, and gE proteins are likely to have key roles in initiating or prolonging the noxious stimulus inducing self-mutilation.

PRV is detected on and within the skin of flank-infected mice. Infectious virus was detected on the skin surface of mice infected with each of the virulent and attenuated PRV strains utilized in the present study (data not shown). Each strain was also shown to replicate within the skin (Fig. 4). Since PRV-Bartha replicated at the site of inoculation (Fig. 4) despite the complete absence of a lesion (Fig. 1B), we conclude that replication within the skin alone is not sufficient to cause a lesion of any kind.

PRV-Becker-infected animals die with very little infectious virus in the brain. PRV first replicates at the site of inoculation and then spreads into the PNS via the sensory and motor nerve endings innervating the skin. In the HSV mouse flank model, infection then spreads from the ganglia out to secondary skin sites within the dermatome (zosteriform spread) (24, 25). To compare the spread of the virulent, mutant, and attenuated PRV strains, various peripheral and CNS tissues were selected at intervals postinoculation for titer assay of infectious virus. Tissues removed included an 8-mm skin punch at the primary site of inoculation, an 8-mm skin punch at a secondary site within the same dermatome, pooled ipsilateral DRG, spinal cord, brain stem tissue, the left hemisphere, and the right hemisphere. The data from the cerebellar tissue were not included since it was difficult to remove the cerebellum without contamination from the brainstem. All other tissues, however, were easily removed without contaminating residues from other tissues.

Tissue titers (PFU/gram of tissue) from mice infected with the virulent strains PRV-Becker, PRV-Kaplan, and PRV-NIA3 were similar (Fig. 4). PRV-NIA3 was the first of the virulent strains detected in the spinal cord (Fig. 4). PRV-Kaplan spread slightly more slowly to secondary skin sites than did PRV-Becker and PRV-NIA3. These virulent strains yielded higher titers than selected mutant strains in samples collected at 36 h. However, by 72 h the titers of virulent virus-infected tissues were reduced in the skin relative to the mutant strains. At 72 h, mice infected with the virulent strains were near death and an abundance of infectious virus was detected in the DRG and spinal cord. The brain samples yielded little to no infectious virus.

High virus loads of PRV-Becker are found within certain visceral organs. A comparison of infectious virus recovered from the visceral organs of mice infected with either PRV-Becker or PRV-Bartha at late stages of infection (70 and 192 h, respectively) yielded the following results (Table 4): minimal amounts of PRV-Becker were detected within heart and lungs, and no infectious virus was recovered from the liver, spleen, or stomach. Substantial titers of PRV-Becker were isolated from the kidneys, adrenal glands, pancreas, ovaries, and pooled urinary bladder and uterine tissue. Infection reaches these organs either (i) by anterograde spread along sympathetic neurons from the lumbar or thoracic spinal cord, (ii) by parasympathic neurons running from lumbar spinal segments through the inferior mesenteric ganglion, or (iii) by retrograde spread from the general

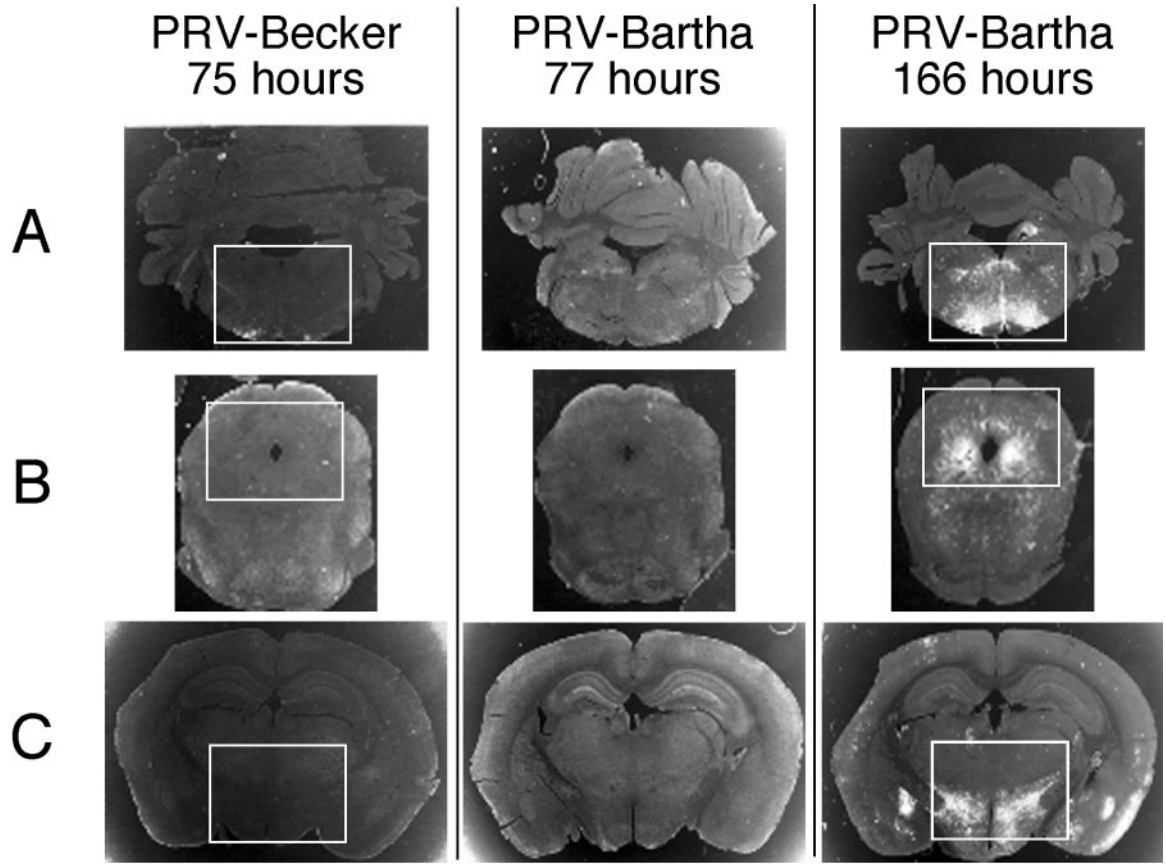

FIG. 5. Immunohistochemical examination of brain sections from mice infected with PRV-Becker and PRV-Bartha. Equivalent anti-PRV stained sections of the hindbrain (A), caudal midbrain (B), and rostral midbrain (C) of mice infected with PRV-Becker at 75 h (moribund stage), PRV-Bartha at 77 h, and 166 h (moribund stage) are shown. Black and white image colors were reversed by using Adobe Photoshop software, and so the viral antigen appears as white. The regions demarcated by rectangles are shown enlarged in Fig. 6.

visceral afferent (GVA) pathways that connect the lumbar spinal cord and the bladder, adrenal glands, and kidneys. These routes of infection in rodents are well characterized (26).

In contrast, the only tissues from PRV-Bartha-infected mice yielding even modest titers of infectious virus were the adrenal glands. PRV-Bartha is likely to reach this tissue solely via through retrograde spread within the GVA pathways. It is noteworthy that visceral organs are only sparsely innervated by GVA neurons, further accounting for the lower levels of PRV-Bartha detected (26).

Attenuated PRV infections reveal an inverse relationship of neuroinvasion and virulence. The tissue distribution of infectious PRV-Bartha particles differed distinctly from the distribution of virulent PRV. The titers were reduced in PRV-Bartha-infected tissues compared to tissues infected with gE-null, gI-null, or U_S9-null mutants at equivalent times postinoculation. Also, entry of PRV-Bartha into each tissue type was delayed. Like PRV-91 (gE-null) and PRV-160 (U_S9-null), PRV-Bartha was not detected at secondary skin sites, as would be predicted if there was no anterograde spread from infected DRG back to skin. In contrast, PRV-98 (gI-null) was detected at secondary skin sites, indicating that the absence of gI exerts only modest effects on anterograde spread from the infected DRG. PRV-Bartha-infected mice survived longer than any other infection, and at these late times infected mice exhibited profound neurological abnormalities. The amount of infectious PRV-Bartha detected in brain tissue at these times exceeded levels detected in brains of virulently infected mice near death by as much as 5 orders of magnitude.

Tissue titers from mice infected with PRV-160 (U_S9-null), PRV-91 (gE-null), and PRV-98 (gI-null) were comparable. The three null mutants were delayed in progression from the skin and through the nervous tissue relative to the virulent strains. At 96 h, mice infected with PRV-160 (U_S9-null), PRV-91 (gE-null), or PRV-98 (gI-null) were near death, and significant titers of infectious virus were recoverable from the brain. The spread from skin to the PNS and to the CNS of PRV-160 (U_S9-null), PRV-91 (gE-null), PRV-98 (gI-null), and PRV-Bartha was delayed relative to the virulent strains. We observed an inverse relationship of neuroinvasiveness to virulence: when virulence (as measured by lesion score and time to death) is reduced, the spread of the virus within the CNS is more extensive.

PRV-Bartha spreads to the brain by efferent and not afferent routes. The skin is innervated by well-known sensory (afferent) and motor (efferent) pathways. Progression to the brain by afferent circuits requires anterograde spread of virus,

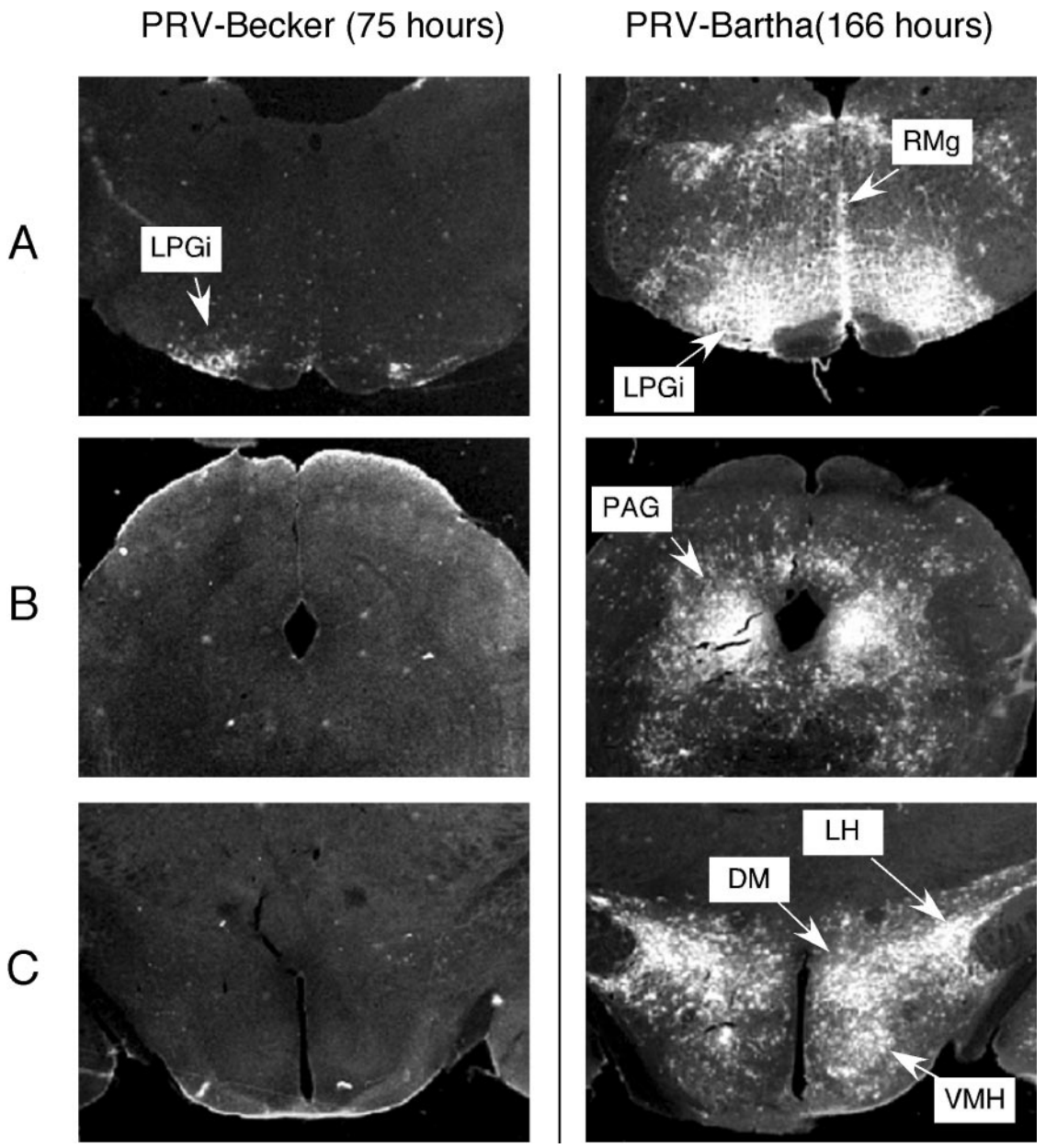

FIG. 6. Magnified regions of anti-PRV-stained sections shown in Fig. 5 (regions demarcated by rectangles). These include hindbrain (A), caudal midbrain (B), and rostral midbrain (C) of mice infected with PRV-Becker at 75 h and PRV-Bartha at 166 h (the respective moribund stages for each infection). Images were reversed in Adobe Photoshop, and so the viral antigen appears as white. Abbreviations: LPGi, lateral paragigantocellular nucleus; DM, dorsomedial hypothalamic nucleus; LH, lateral hypothalamic area; VMH, ventromedial hypothalamic nucleus.

whereas movement through efferent circuits requires retrograde spread.

At 75 h, when PRV-Becker-infected animals were in the final stages of the disease, animals were sacrificed and perfused with paraformaldehyde by transcardiac perfusion. The brains were subsequently harvested for immunohistochemical analysis. Brains from PRV-Bartha-infected mice were also removed at 77 h for comparison as well as at 166 h (Fig. 5 and 6). At ca. 75 to 77 h, little viral antigen was detectable in the brains of mice infected with either PRV-Becker or PRV-Bartha (Fig. 5). This is consistent with the tissue titer data shown in Fig. 4. Small quantities of viral antigen can be detected in the brainstem but not the in the cerebellum in hindbrain sections of some PRV-Becker-infected mice. No antigen was detected in midbrain or forebrain sections. The regions infected in the brainstems of PRV-Becker-infected animals at 75 h include the lateral paragigantocellular nucleus (Fig. 5 and 6). The amount of infectious PRV-Becker in the brainstem at 75 to 77 h is greater relative to PRV-Bartha at the equivalent time point, when little to no virus has reached the brain.

Viral antigen was barely detectable in the brains of some PRV-Becker-infected animals in the moribund stage of infection. In contrast, many areas of the brains in all PRV-Bartha-infected animals near death contained an abundance of viral

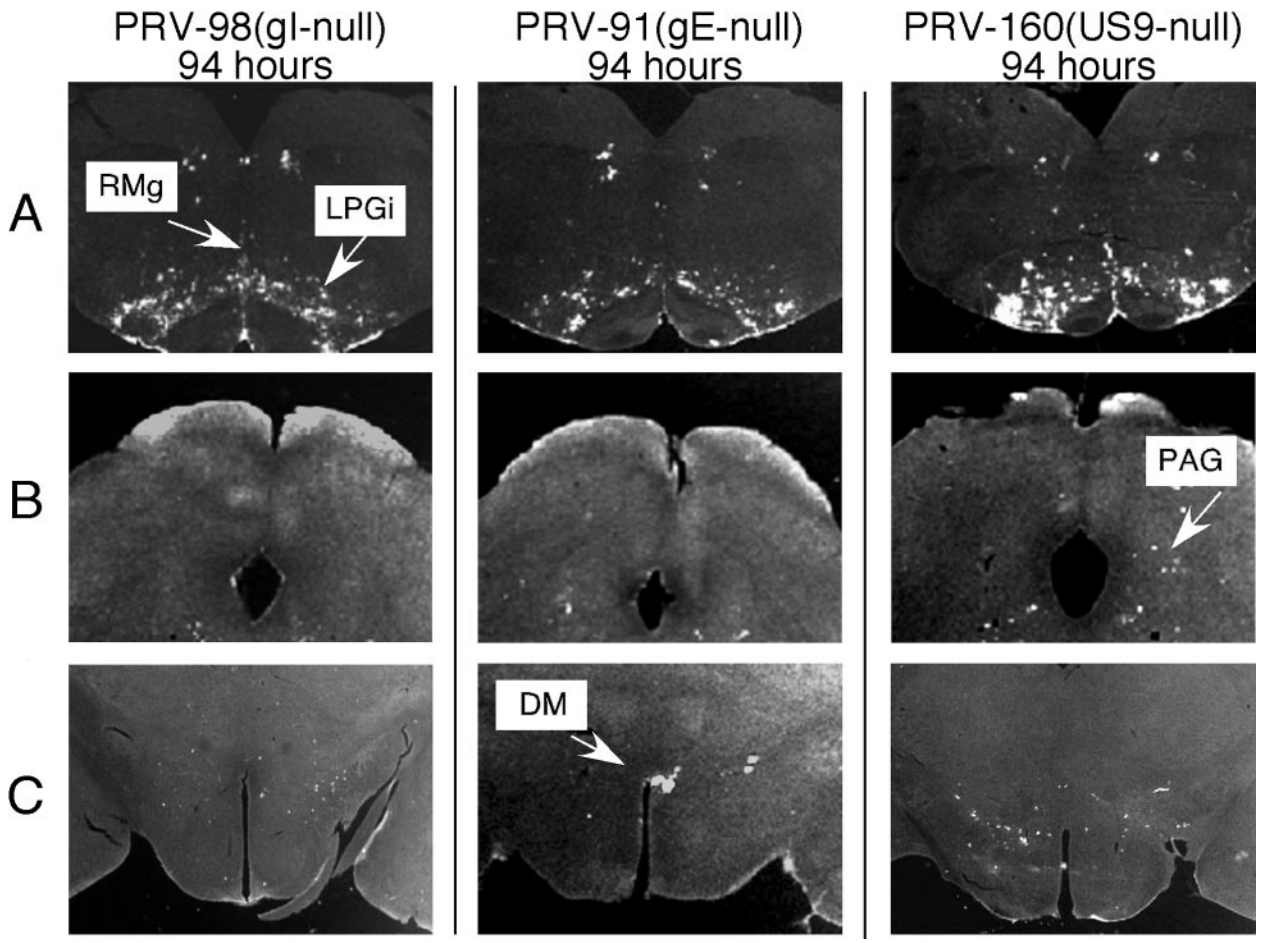

FIG. 7. Images of equivalent sections of hindbrain (A), caudal midbrain (B), and rostral midbrain (C) of mice infected with PRV-98 (gI null), PRV-91 (gE null), and PRV-160 (U_S9 null) at 94 h (advanced morbidity). Images were reversed in Adobe Photoshop, and so viral antigen appears as white. The intense white appearance at the edge of the sections is an artifact of tissue staining. Abbreviations: LPGi, lateral paragigantocellular nucleus; DM, dorsomedial hypothalamic nucleus.

antigen (Fig. 5 and 6). The infected areas of the brain correspond to the major efferent (motor) centers that define the descending serotonergic-opioid analgesic pathway to the skin. These include the raphe magnus nucleus (RMg) of the brainstem and the periaqueductal gray (PAG) of the midbrain. The primary motor cortex of the forebrain also contained PRV-Bartha antigen. These results support our hypothesis that PRV-Bartha can only spread in the retrograde direction in neuronal circuits (20).

At 94 h, when mice infected with PRV-98 (gI null), PRV-91 (gE null), or PRV-160 (U_S9 null) were in the late stages of disease, comparable amounts of viral antigen were detected by immunohistochemistry (Fig. 7). The areas where viral antigen was detected correspond to the RMg, PAG, and the dorsomedial hypothalamic nucleus. These areas contained less viral antigen than that observed in PRV-Bartha-infected brains late in the course of the disease. No viral antigen was detected in the cerebellum of any brains analyzed.

Tracing two modes of neuroinvasion by PRV. The sensory neurons in the DRG that receive input from skin structures project axons to the dorsal horn of the spinal cord. In contrast, motor neurons in the ventral horn of the spinal cord project axons out to the skin. We hypothesized that virulent PRV would be capable of spread from the spinal cord to the brain by both afferent and efferent routes and therefore that both efferent and afferent centers of the spinal cord would contain viral antigen. In contrast, PRV-Bartha would spread only by efferent routes resulting in infection of only the efferent centers of the spinal cord.

We used immunohistochemical analysis to examine serial sections of the lumbar and thoracic regions of spinal cords from mice infected with PRV-Becker (at 72 h) and PRV-Bartha (at 96 h). Selected sections are shown in Fig. 8. These time points were chosen because virus recovered was approximately equal (10^5 PFU/g) for both PRV-Becker-infected mice at 72 h and PRV-Bartha-infected mice at 96 h. In the lumbar region, the portion of the spinal cord receiving direct innervation from the primary infected ganglia, antigen was detected primarily in the dorsal horn (the site of sensory input) of PRV-Becker-infected mice. Staining of the ventral horn (the site of motor input) can also be detected in lumbar spinal cord sections from PRV-Becker-infected mice. The PRV-Bartha-infected lumbar spinal cord sections yielded intense staining of an efferent column (the intermediolateral cell column) with

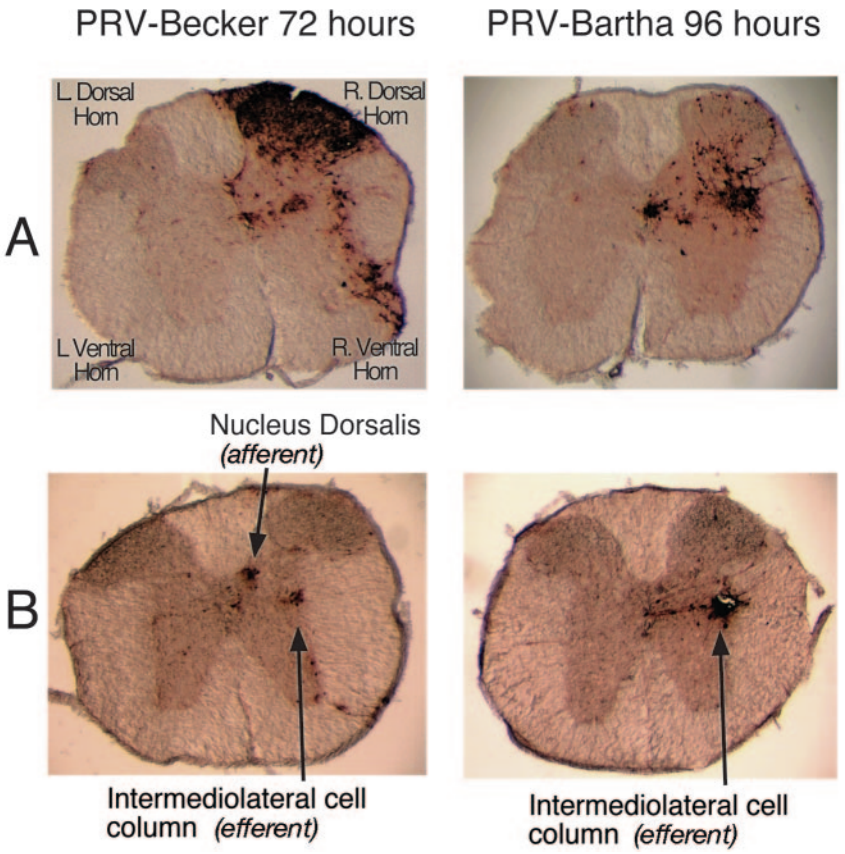

FIG. 8. Images of sections of lumbar (A) and thoracic (B) spinal cord sections harvested from PRV-Becker-infected mice at 72 h or PRV-Bartha-infected mice at 96 h. Sections are stained for PRV antigen, which appears as dark brown. Left and right dorsal and ventral horns are labeled for orientation.

staining of some neurons within the dorsal horn. Presumably, PRV-Bartha spreads from motor neurons to sensory centers within the lumbar region through retrograde spread along interneurons.

To verify that PRV-Becker spread was occurring along both efferent and afferent routes and that PRV-Bartha spread only via efferent pathways, thoracic spinal cord sections were also analyzed. PRV-Becker antigen was detected within the nucleus dorsalis (or "column of Clarke" containing afferent collaterals), as well as within the intermediolateral cell column. This indicated that spread occurs in both anterograde and retrograde fashions. PRV-Bartha antigen, however, was detected only in the intermediolateral cell column, indicating that spread to the brain occurred solely by retrograde spread.

DISCUSSION

The classic mouse flank infection model of HSV described by Simmons and Nash described a primary lesion at the site of inoculation 2 days postinfection, followed by secondary lesions (zosteriform vesicles) along the dermatome at approximately 4 days postinfection (25). The primary lesions result from host response to viral replication. HSV then invades sensory neurons innervating the skin (neurons of the DRG). Motor neurons originating in the ventral horn of the spinal cord projecting to the skin are also infected. Similarly, motor neurons of sympathetic ganglia, peripheral ganglia distinct from DRG that innervate the skin, also are infected. In the original flank infection model, HSV spreads to sensory DRG neurons in the primary infection and then spreads back to all of the skin sites innervated by the infected DRG neurons (the dermatome innervated by the DRG). The resulting secondary lesions were vesicular and were reminiscent of herpes zoster lesions (shingles), hence the term "zosteriform rash." Depending on the strain and inoculating dose, 30 to 60% of HSV-infected mice survive infection (29).

The outcome of infection in the present model with PRV is strikingly different. The main points of difference are as follows. Wild-type PRV-infected animals exhibit a dramatic peripheral neuropathy that results in self-mutilation due to violent scratching and biting of the afflicted dermatome. Even when self-mutilation is blocked by anesthesia, animals still die at the same time as alert animals that exhibit violent scratching behavior. Initially, we thought that vesicular lesions, if present, were completely obscured by the dramatic skin damage. However, this cannot be the case, for in the absence of self-mutilation, no lesions of any severity were evident, despite evidence of viral replication in the skin.

Contrast between neuroinvasion and direct infection of the CNS. A PRV strain that can spread from a site in the host

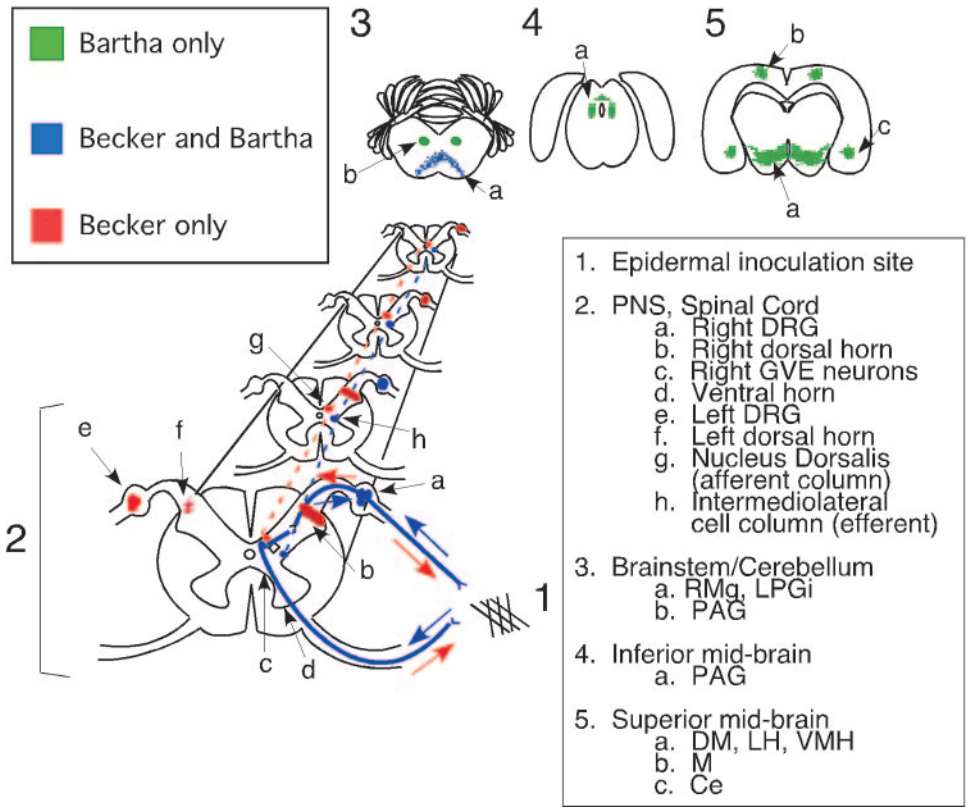

FIG. 9. Schematic diagram of spread of PRV-Becker and PRV-Bartha in the mouse flank scarification infection model. Abbreviations: GVE, general visceral efferent; LPGi, lateral paragigantocellular nucleus; DM, dorsomedial hypothalamic nucleus; LH, lateral hypothalamic area; VMH, ventromedial hypothalamic nucleus; M, motor cortex; Ce, central amygdaloid nucleus.

periphery to the CNS is described as neuroinvasive. Infection models that involve structures of the head, neck, and viscera (eyes, ears, mouth, nose, or peritoneal infection) expose the cranial nerves to infection (1, 2, 6, 28). Some cranial neurons reside in the brain and spinal cord and send axons outside the CNS to peripheral sites. Axon terminals of these neurons can be directly infected from the periphery, resulting in the spread of infection to the CNS within a single neuron. Similarly, neurons of other cranial nerves relay sensory information to the brain (e.g., the trigeminal, optic, and olfactory nerves). These neurons have their cell bodies outside the CNS and project axons into the CNS. In some cases, the cell bodies can be infected and virions can spread directly into the brain (e.g., retinal ganglion cells and olfactory neurons).

If neuroinvasiveness is measured by the presence of viral antigen or infectious virus in the brain, the measurement can reflect two distinct types or combinations of neuronal infection: infection of primary neurons in cranial nerves or transneuronal spread of infection from peripheral ganglia to the CNS. These properties are distinctive because the former reflects movement inside a single neuron and movement across a single synapse into the CNS. The latter requires not only long distance movement within neurons but also the spread of infection across several types of specialized cell-cell junctions. Assertions whether viral mutants are neuroinvasive or not must be qualified by noting which types of neurons are infected. In the flank model, all assignments of neuroinvasiveness require that infection spread from the epithelia into the PNS and then into the CNS. Moreover, given the physical distance required for the infection to spread from the flank to the brain, temporal separation of phenotypes resulting from PNS and CNS invasion is possible. Accordingly, we are able to discern two modes of neuroinvasion for PRV.

Two modes of neuroinvasion and lethality. Virulent PRV can enter the CNS by efferent and afferent routes, whereas PRV-Bartha enters exclusively by efferent routes (Fig. 9). PRV-Becker enters the CNS through both ascending sensory pathways and the corresponding paired descending inhibitory pathways of the endogenous neuromodulatory system. PRV-Bartha enters the CNS exclusively through efferent routes such as the descending serotonergic-opioid analgesic pathway, which normally serves to modulate sensations of pain. This analgesic pathway descends from the PAG of the midbrain to the nucleus RMg of the brainstem into the dorsolateral funiculus of the spinal cord and finally to the site of innervation within the epidermis. The presence of viral antigen in these areas after PRV-Bartha infection corresponds precisely to this autonomic pathway. PRV-Becker antigens can occasionally also be detected in neurons of the serotonergic-opiod analgesic pathway during the moribund stage of infection, but to a much lower extent than PRV-Bartha.

Very little infectious virus can be detected within, or isolated from, the brains of mice infected with PRV-Becker compared to PRV-Bartha. Therefore, we suggest that a virulent flank

infection does not kill by brain infection. Other factors that trigger the early death of virulently infected mice may be absent or reduced in animals infected with the highly attenuated PRV-Bartha vaccine strain, allowing much more extensive neuroinvasion to occur. The flank scarification model has enabled separation of these lethal effects with the potential to identify the corresponding viral genes required.

Our finding that PRV-Bartha invades the CNS by efferent routes confirms the findings from circuit tracing studies demonstrating that PRV-Bartha spreads unidirectionally (retrograde spread) in the neuronal circuits of a variety of experimental animal models (20). We have also demonstrated that the anterograde-spread defect of PRV-Bartha is applicable to the neurons of the PNS (including the pseudo-unipolar neurons of the DRG) as well as the CNS. These two modes of neuroinvasion result in different sets of infected neurons in the CNS and two different lethal syndromes. We now understand that the general basis for this discriminatory neuroinvasiveness is based on the function of at least three PRV gene products: gE, gI, and U_S9. Deletion of either the gE gene or the U_S9 gene results in the inability of infection to spread through afferent pathways, whereas deletion of the gI gene markedly reduces this spread.

Since symptoms of infection are greatly reduced and early death is avoided, attenuated viruses spread to the CNS, producing a characteristic delayed syndrome of behavioral and motor abnormalities and ultimately death. U_S9, gI, and gE each contribute to virulence, but the relationship of their role in neuroinvasion to virulence remains to be explained (4, 15).

Pruritus results from PNS not CNS infection. The infection of sensory routes by virulent PRV includes the characteristic symptoms and early death in nonnative animals that gave the disease its common name, "pseudorabies." We suggest that these hallmark signs of pruritus and the rapid lethality reflect infection of the sensory arm of PNS and not the brain. It is likely that virulent infection of the sensory ganglia, facilitated by the products of the genes encoding gE, gI, and U_S9, plays a major role in the virulent PRV syndrome.

The noxious stimulus provoking the uncontrolled scratching and biting most likely emanates from the infected DRG because the lesions define precise dermatomes, and infectious virus is detected in abundance in this tissue during the times when pruritus is observed. At these times, no viral antigen or infectious virus is detected in the brain. This idea was also offered by Takahashi et al. based on their proposal that the characteristic pruritus associated with PRV is associated with the invasion of the trigeminal ganglion after a subcutaneous infection of mouse forelimbs (27). The pruritic stimulus is mediated, at least in part, by gE, gI, and U_S9 proteins, since infection with gE-, gI-, and U_S9-null mutants resulted in reduced pruritus and diminished lesion severity from self-mutilation.

It is not clear why pruritus is essentially absent in HSV mouse skin infections, even though HSV has homologues to gE, gI, and U_S9. However, PRV-induced pruritus is reminiscent of the pain and itching experienced by humans during varicella-zoster virus reactivation (shingles) or in clinical cases of herpes whitlow (11). Analysis of the PRV model may help elucidate the root causes of pruritus and postherpetic neuralgia, for which there are few animal models available.

ACKNOWLEDGMENTS

We are grateful to Marlies Eldridge of the Enquist laboratory (Princeton University) for invaluable advice and assistance with immunohistochemical techniques. We thank Pat Card (University of Pittsburgh) for expert assistance in defining the neuroanatomic structures infected with PRV and the routes of infection in the nervous system. We gratefully acknowledge John Lubinski of the Friedman laboratory (University of Pennsylvania) for providing training in techniques used in the mouse flank model of viral pathogenesis. We thank Tony Simmons (University of Texas Medical Branch) for his suggestion to use the mouse flank scarification model to study PRV. Bruce Banfield (University of Colorado) kindly provided PRV-158. Saul Silverstein and Jennifer Schwartz (Columbia University) provided key insight and assistance in early stages of the analysis of the PRV skin lesions. Trisha Barney (Princeton University) offered excellent administrative support. Members of the Princeton University Animal Care Facility provided excellent care and assistance in maintaining the animals used for these studies.

This study was supported by NIH NINDS grant R0133506 to L.W.E.

REFERENCES

1. **Babic, N., B. Klupp, A. Brack, T. C. Mettenleiter, G. Ugolini, and A. Flamand.** 1996. Deletion of glycoprotein gE reduces the propagation of pseudorabies virus in the nervous system of mice after intranasal inoculation. Virology **219:**279–284.
2. **Banfield, B. W., G. S. Yap, A. C. Knapp, and L. W. Enquist.** 1998. A chicken embryo eye model for the analysis of alphaherpesvirus neuronal spread and virulence. J. Virol. **72:**4580–4588.
3. **Bartha, A.** 1961. Experimental reduction of virulence of Aujeszky's disease virus. Mag. Allat. Lap. **16:**42–45.
4. **Brideau, A. D., J. P. Card, and L. W. Enquist.** 2000. Role of pseudorabies virus Us9, a type II membrane protein, in infection of tissue culture cells and the rat nervous system. J. Virol. **74:**834–845.
5. **Card, J. P., and L. W. Enquist.** 1999. Transneuronal circuit analysis with pseudorabies virus. Curr. Prot. Neurosci. **1.5:**1–28.
6. **Card, J. P., L. Rinaman, J. S. Schwaber, R. R. Miselis, M. E. Whealy, A. K. Robbins, and L. W. Enquist.** 1990. Neurotropic properties of pseudorabies virus: uptake and transneuronal passage in the rat central nervous system. J. Neurosci. **10:**1974–1994.
7. **Card, J. P., M. E. Whealy, A. K. Robbins, and L. W. Enquist.** 1992. Pseudorabies virus envelope glycoprotein gI influences both neurotropism and virulence during infection of the rat visual system. J. Virol. **66:**3032–3041.
8. **Enquist, L. W.** 2002. Exploiting circuit-specific spread of pseudorabies virus in the central nervous system: insights to pathogenesis and circuit tracers. J. Infect. Dis. **186**(Suppl. 2)**:**S209–S214.
9. **Enquist, L. W.** 1999. Life beyond eradication: veterinary viruses in basic science. Arch. Virol. Suppl. **15:**87–109.
10. **Enquist, L. W., R. R. Miselis, and J. P. Card.** 1994. Specific infection of rat neuronal circuits by pseudorabies virus. Gene Ther. **1:**S10.
11. **Gilden, D. H., R. J. Cohrs, and R. Mahalingam.** 2003. Clinical and molecular pathogenesis of varicella virus infection. Viral Immunol. **16:**243–258.
12. **Husak, P. J., T. Kuo, and L. W. Enquist.** 2000. Pseudorabies virus membrane proteins gI and gE facilitate anterograde spread of infection in projection-specific neurons in the rat. J. Virol. **74:**10975–10983.
13. **Klupp, B. G., C. J. Hengartner, T. C. Mettenleiter, and L. W. Enquist.** The complete annotated sequence of the pseudorabies virus (PRV) genome. J. Virol. **78:**424–440.
14. **Klupp, B. G., B. Lomniczi, N. Visser, W. Fuchs, and T. C. Mettenleiter.** 1995. Mutations affecting the UL21 gene contribute to avirulence of pseudorabies virus vaccine strain Bartha. Virology **212:**466–473.
15. **Knapp, A. C., P. J. Husak, and L. W. Enquist.** 1997. The gE and gI homologs from two alphaherpesviruses have conserved and divergent neuroinvasive properties. J. Virol. **71:**5820–5827.
16. **Lomniczi, B., S. Watanabe, T. Ben-Porat, and A. S. Kaplan.** 1987. Genome location and identification of functions defective in the Bartha vaccine strain of pseudorabies virus. J. Virol. **61:**796–801.
17. **Lyman, M. G., G. L. Demmin, and B. W. Banfield.** 2003. The attenuated pseudorabies virus strain Bartha fails to package the tegument proteins Us3 and VP22. J. Virol. **77:**1403–1414.
18. **Mettenleiter, T. C., N. Lukacs, and H. J. Rziha.** 1985. Pseudorabies virus avirulent strains fail to express a major glycoprotein. J. Virol. **56:**307–311.
19. **Petrovskis, E. A., J. G. Timmins, T. M. Gierman, and L. E. Post.** 1986. Deletions in vaccine strains of pseudorabies virus and their effect on synthesis of glycoprotein gp63. J. Virol. **60:**1166–1169.
20. **Pickard, G. E., C. A. Smeraski, C. C. Tomlinson, B. W. Banfield, J. Kaufman, C. L. Wilcox, L. W. Enquist, and P. J. Sollars.** 2002. Intravitreal injection of the attenuated pseudorabies virus PRV Bartha results in infection of the hamster suprachiasmatic nucleus only by retrograde transsynaptic transport via autonomic circuits. J. Neurosci. **22:**2701–2710.

21. **Reed, L. J., and H. Muench.** 1938. A simple method of estimating fifty per cent endpoints. Am. J. Hyg. **27:**493–497.
22. **Robbins, A. K., J. P. Ryan, M. E. Whealy, and L. W. Enquist.** 1989. The gene encoding the gIII envelope protein of pseudorabies virus vaccine strain Bartha contains a mutation affecting protein localization. J. Virol. **63:**250–258.
23. **Roizman, B.** 1990. *Herpesviridae*: a brief introduction, p. 1787–1793. *In* B. N. Fields, D. M. Knipe, and P. M. Howley (ed.), Fields virology, 3rd ed. Lippincott-Raven Publishers, Philadelphia, Pa.
24. **Saldanha, C. E., J. Lubinski, C. Martin, T. Nagashunmugam, L. Wang, H. van Der Keyl, R. Tal-Singer, and H. M. Friedman.** 2000. Herpes simplex virus type 1 glycoprotein E domains involved in virus spread and disease. J. Virol. **74:**6712–6719.
25. **Simmons, A., and A. A. Nash.** 1984. Zosteriform spread of herpes simplex virus as a model of recrudescence and its use to investigate the role of immune cells in prevention of recurrent disease. J. Virol. **52:**816–821.
26. **Strack, A. M., W. B. Sawyer, L. M. Marubio, and A. D. Loewy.** 1988. Spinal origin of sympathetic preganglionic neurons in the rat. Brain Res. **455:**187–191.
27. **Takahashi, H., Y. Yoshikawa, C. Kai, and K. Yamanouchi.** 1993. Mechanism of pruritus and peracute death in mice induced by pseudorabies virus (PRV) infection. J. Vet. Med. Sci. **55:**913–920.
28. **Tirabassi, R. S., R. A. Townley, M. G. Eldridge, and L. W. Enquist.** 1998. Molecular mechanisms of neurotropic herpesvirus invasion and spread in the CNS. Neurosci. Biobehav. Rev. **22:**709–720.
29. **Weeks, B. S., R. S. Ramchandran, J. J. Hopkins, and H. M. Friedman.** 2000. Herpes simplex virus type-1 and -2 pathogenesis is restricted by the epidermal basement membrane. Arch. Virol. **145:**385–396.
30. **Whealy, M. E., J. P. Card, A. K. Robbins, J. R. Dubin, H. J. Rziha, and L. W. Enquist.** 1993. Specific pseudorabies virus infection of the rat visual system requires both gI and gp63 glycoproteins. J. Virol. **67:**3786–3797.
31. **Wittmann, G., and H. J. Rziha.** 1989. Aujeszky's disease (pseudorabies) in pigs, p. 230–333. *In* G. Wittmann (ed.), Herpesvirus diseases of cattle, horses, and pigs. Kluwer Academic, Boston, Mass.
32. **Yang, M., J. P. Card, R. S. Tirabassi, R. R. Miselis, and L. W. Enquist.** 1999. Retrograde, transneuronal spread of pseudorabies virus in defined neuronal circuitry of the rat brain is facilitated by gE mutations that reduce virulence. J. Virol. **73:**4350–4359.